Macromolecules
COMMUNICATION TO THE EDITOR

Macromolecules **2009**, *42*, 3877–3880 **3877**
DOI: 10.1021/ma900485q

Controlled Photooxidation of Nanoporous Polymers

Sokol Ndoni,*,† Li Li,†,‡ Lars Schulte,†,‡ Piotr P. Szewczykowski,†,‡ Thomas W. Hansen,§ Fengxiao Guo,†,‡ Rolf H. Berg,† and Martin E. Vigild*,‡

†*Department of Micro- and Nanotechnology, Technical University of Denmark, DK-4000 Roskilde, Denmark,* ‡*Department of Chemical and Biochemical Engineering Technical University of Denmark, DK-2800 Kgs. Lyngby, Denmark, and* §*Center for Electron Nanoscopy, Technical University of Denmark, DK-2800 Kgs. Lyngby, Denmark*

Received March 5, 2009
Revised Manuscript Received May 3, 2009

The general phenomenon of photooxidation[1−5] involves oxygen gas permeation[6,7] into the material under photochemical reaction, typically mediated by UV radiation. It has been extensively studied mainly driven by material degradation concerns.[1−5] The effects of photooxidation to the emerging class of nanoporous polymers[8−14] (NP) are unexplored and hold great potential for both the fundamental understanding of polymer photooxidation in general and for nanotechnological applications. Uses of NP as ultrafiltration membranes[10] or as cladding for liquid core wave guides[12] are worth mentioning in the context of the present work. Nanoporous polymers derived from self-organized block copolymers[15] show crystalline-like order with typical structural length scales in the range 10−100 nm; they have vast internal surfaces (50−500 $m^2\ g^{-1}$), which in the presence of pore percolation are readily accessible to gases. For structural length scales much smaller than the wavelength of UV-A, B radiation ($\lambda > 280$ nm), radiation penetration depth is not seriously limited by scattering.[16] No experimental or modeling report was found on the photooxidative stability of nanoporous polymers. One report describes treatment of a nonpolymeric matrix[17] with UV-254 nm and ozone; the survival of nanoporosity was uncertain.

We demonstrate that the polymer−air interface of nanoporous polymers can be altered by controlled photooxidation in air, without compromising nanostructure. Patterned hydrophilicity can be generated, spawning interesting applications. We also illustrate, by the straightforward calculation of the oxygen fixation quantum yield,[1,2] that NP open new possibilities for fundamental surface studies of polymers. The effect of photooxidation is described here for the case of nanoporous cross-linked 1,2-polybutadiene[18] of gyroid morphology[19] derived from a self-assembled 1,2-polybutadiene-*b*-polydimethylsiloxane (PB−PDMS) diblock copolymer. The conceptual scheme of the present contribution is shown in Figure 1. Figure S1 of the Supporting Information demonstrates the nanoporosity-enhanced photooxidation of another polymer, polystyrene.

PB−PDMS was prepared by "living" anionic polymerization.[20] The number-average molecular mass of the 1,2-PB block was 6300 g mol^{-1} and its mass fraction 0.59. The 1,2-PB microphase was first cross-linked at 140 °C for 2 h under argon, and then PDMS was specifically and quantitatively removed by tetrabutylammonium fluoride, following our recently reported procedure.[18] Either aromatic dicumyl peroxide or aliphatic diamyl peroxide was used as free radical generators at 1% molar concentration relative to the PB repeating units. 0.50 mm NP films were photooxidized in air at either 32 ± 2 or 42 ± 2 °C, for times of up to 50 h by UV generated from Philips Cleo 25W RS UV lamps. Lithographic masks were used for micropatterning, while the coarser masks were machined on aluminum sheets. The radiation wavelength range chosen for the modification of *x*-PB was 310−420 nm, peaking at 350 nm; the radiant flux at the samples' position was measured to 31 ± 2 mW cm^{-2}. Finally, copper electrotemplating was realized at 40 V at an electrode separation of 20 mm from 1 M copper(II) chloride solution (see Figure 4c).

Figure 2a−d shows transmission electron microscopy (TEM) images of the NP after 0, 10, 30, and 40 h of UV treatment. The morphology is conserved in the time window as confirmed by small-angle X-ray scattering (SAXS) (Figure 2e). The equality of length scales shown by SAXS indicates that oxygen photofixation for irradiation times of up to 40 h mainly happens at the polymer−air interface.[21−23]

The sample dry mass increases with irradiation time due to oxygen fixation as plotted in Figure 3a. After 50 h of irradiation the mass increases by 21% relative to the nanoporous native sample. Figure 3b shows the equilibrium value for water uptake of samples submerged in water after increasing UV-irradiation times. The sigmoid trend shows that there is a lower limit of roughly 6−8 h in irradiation time before spontaneous wetting can start. This can be interpreted as the time needed to reach a critical value for the surface density of the generated hydrophilic groups. At 30 h the water uptake is 0.63 ± 0.03, which together with the dry oxidation mass adds up to a total volume fraction of 0.44 ± 0.02 (1 g cm^{-3} overall density assumed). The pore volume fraction of the original NP as measured by methanol uptake is 0.43 ± 0.01, nicely matching the above value and reconfirming structure stability. For the samples irradiated at 40 and 50 h the total volume fraction of absorbed water and fixed oxygen exceeds by up to 7% the pore volume fraction of the original NP, probably due to slight sample swelling in water. Detailed analyses of the results are complicated by the depth gradient of sample photooxidation degree.

The effects of temperature and cross-linking agent on the photooxidation reaction were tested by operating at two temperatures (32 and 42 °C) and with two cross-linkers (one aromatic and one aliphatic peroxide).[24] Within experimental uncertainty samples irradiated at 32 and 42 °C cannot be discriminated by the data in Figure 3a. However, Figure 3b hints to a sharper "hydrophilic transition" taking place at the lower temperature. The effect of temperature on the sharpness of the transition is more evident in Figure S3, where the *x*-axis is the absorbance at 350 nm. The lower temperature therefore favors the formation of hydrophilic groups at the polymer−air interface throughout the sample thickness. A more systematic study of the effect of temperature in the range 0−50 °C is in progress.

The distinctive possibilities the present materials open for fundamental studies of photooxidation of polymers in general is illustrated below by the calculation of the initial oxygen fixation quantum yield,[1,2] $\overline{Q^0_{O_2}}$, which is the wavelength averaged probability for an absorbed photon to create a covalent bond between polymer and oxygen:

$$\overline{Q^0_{O_2}} = \left(\frac{dN_{O_2,\,fix}}{dN_{h\nu,\,abs}}\right)_{time=0} = \left(\frac{dN_{O_2,\,fix}/dt}{dN_{h\nu,\,abs}/dt}\right)_{t=0}; \quad 310\ nm < \lambda < 400\ nm$$

*Corresponding authors. E-mail: sokol.ndoni@nanotech.dtu.dk (S.N.); mev@kt.dtu.dk (M.E.V.).

Published on Web 05/19/2009

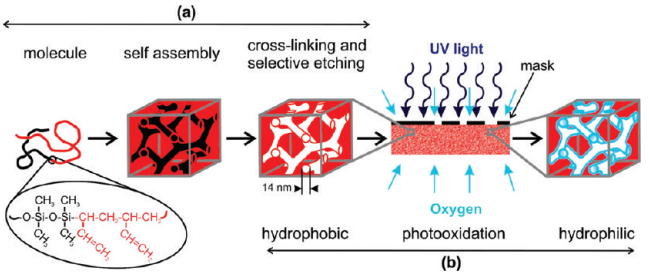

Figure 1. Conceptual scheme showing (a) preparation of a cross-linked nanoporous polymer of gyroid morphology from a self-assembled diblock copolymer and (b) controlled photofixation of oxygen onto the pore walls. Hydrophilic patterns can be created by application of UV masks. The polymer matrix (red zone) constitutes the pore walls (0.57 volume fraction, 20−30 nm thick). The wall volume separated ~1 nm from the air−polymer interface is referred to as "polymer bulk" in the text.

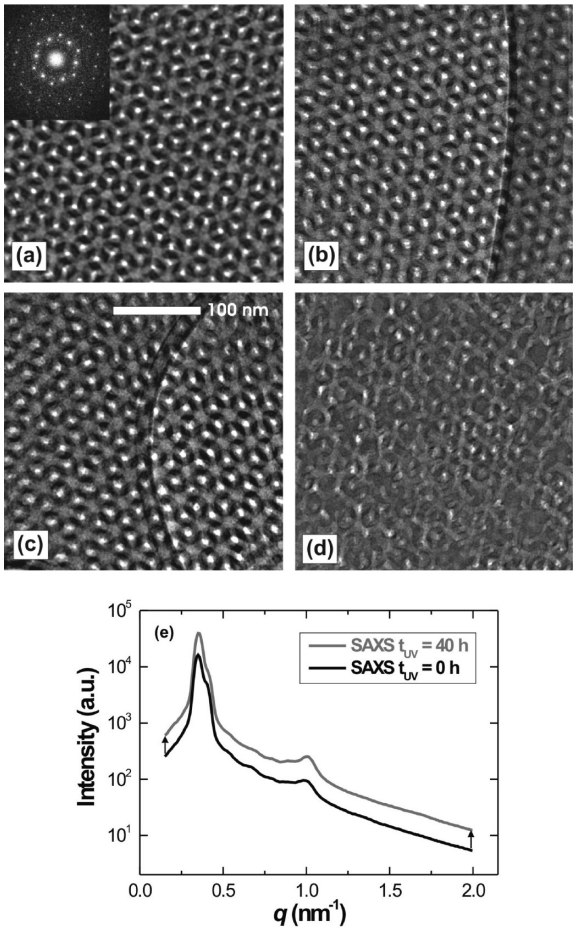

Figure 2. Structural characterization by TEM and SAXS of nanoporous *x*-PB after (a) 0, (b) 10, (c) 30, and (d) 40 h of UV treatment. The "wagon wheel" (111) projection of the gyroid structure is neatly visible in all the TEM micrographs. The light regions correspond to the interconnected porous structure of tripod struts with the white spots marking the struts with highest projected porosity. The inset in (a) is a fast Fourier transform of the image illustrating the high degree of order. The micrograph (d) shows less regularity than the other three; we argue that this is not due to loss of nanoporous morphology but probably to sample brittleness caused by inhomogeneous oxidation at different depths. TEM specimen preparation becomes difficult for such samples, resulting in fractured microtomed surface at the scale of the micrographs. The preservation of morphology is directly supported by the similarity of the SAXS profiles after 0 and 40 h of UV irradiation shown in (e). For most applications modification depths 10−100 times smaller than the present sample thickness will be of interest; in such cases irradiation times of 8−15 h will be sufficient at equal UV intensity.

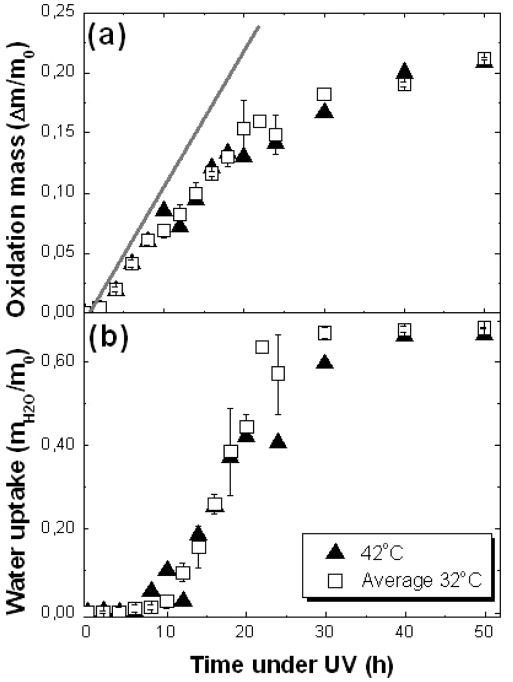

Figure 3. Mass change due to oxygen photofixation and equilibrium of water uptake as a function of UV irradiation time and temperature. (a) Degree of oxygen fixation expressed as dry mass increase relative to the unmodified samples for three sets of samples irradiated at 32 °C and one set at 42 °C. The straight line marks the initial slope of the mass growth used to calculate the O_2-fixation quantum yield. (b) Equilibrium water uptake of samples treated at different times by UV-350 nm. The increase of water uptake after 8 h of UV treatment is due to an increased volume of the NP sample being rendered hydrophilic starting from the side directly exposed to UV. After 22−30 h the whole sample of thickness 0.50 mm is rendered hydrophilic.

$N_{O_2,fix}$ and $N_{h\nu,abs}$ are the number of O_2 molecules covalently bond to the polymer and the number of photons absorbed by the NP, respectively. The numerator in the last expression can be readily evaluated from the initial slope in Figure 3a; the denominator is calculated from the polymer transmission UV spectrum at time $t = 0$ and the lamp emission profile, as illustrated in Figure S2 of the Supporting Information. The possibility to calculate $\overline{Q^0_{O_2}}$ (0.24 ± 0.03, no literature value could be found for comparison) by using an analytical balance is directly related to the concentrated interface area and the high oxygen permeability in the nanoporous samples. Accurate mapping of the $Q^0_{O_2}$ dependence on λ is possible by using monochromatic radiation of known wavelength. Other important parameters, difficult to obtain in other ways, such as the kinetics of photooxidation and the type and distribution of the generated chemical groups can be gained by the present procedure.

The ability of the UV-modified samples to take up water remained unchanged for at least 6 months, during which dry samples stored under argon for the period behaved in the same way as freshly UV-irradiated ones.[25] This is an attractive feature since many hydrophilically modified polymers show irreversible hydrophobic recovery[26] after few days of storage in the dry state.

Figure 4 illustrates the UV patterning of the hydrophobic matrix and two derived applications on wave guiding and metal nanotemplating. Patterning of hydrophilic regions into hydrophobic surrounding is straightforward by utilizing appropriate masks. Fine patterns in the micrometer scale were fabricated, as shown in Figure 4a (see also Figure S4). The spatial decorations realized here are fascinating as they are a convolution of nanoporosity into micropatterns. When submerged into water such samples wet exclusively in the irradiated zones. The added water increases the refractive index in the hydrophilic regions,

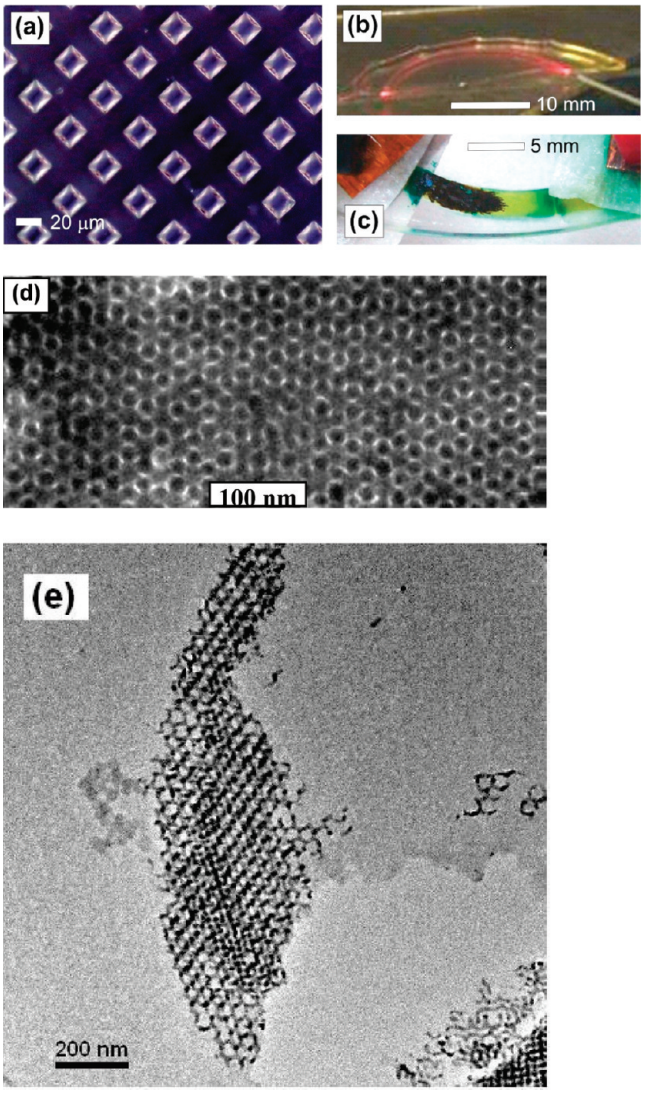

Figure 4. Examples of NP with added functionality by photooxidative decoration. (a) Grid of hydrophilic squares of size 20 μm in a 2-D square lattice of 40 μm principal distance (for a 5 μm feature pattern see Figure S4). The wet patterned NP was placed between two microscope glasses in order to prevent water evaporation. The presence of water exclusively in the hydrophilic regions gives rise to an increased contrast of refractive indices between the two zones. (b) Demonstration of principle of 630 nm laser light guiding along a wet nanoporous zone formed as a 140° arch of 1 mm width and 0.3 mm depth. The light source (laser light passing through a syringe needle of 0.8 mm opening) is visible at the right bottom corner. (c) Copper electrodeposition along a 2.0 mm wide hydrophilic zone surrounded by hydrophobic nanoporous polymer. (d) TEM image from the metal filled zone (Figures S6 and S7 show a high-resolution TEM of the template). (e) TEM of template "finger" with visible gyroid copper scaffold.

providing picture contrast under the optical microscope. Again, the refractive index contrast allows light guiding at total internal reflection, as demonstrated in Figure 4b.[27]

Figure 4c shows directed electrodeposition of copper through a 2 mm wide and 0.5 mm thick hydrophilic strip (cathode on the left; both electrodes embrace the NP sample through copper sheets and filter paper helping to keep the sample extremities wet). The growing finger pattern of the nanotemplated (black) copper on the cathode (left) is evident. Nanotemplating was confirmed by SAXS (not shown), by TEM shown in Figure 4d,e, and by high-resolution TEM shown in Figures S5 and S6. The conservation of the gyroid morphology after electrotemplating is evident from Figure 4d,e. The hydrophilic nanopores are filled with copper which is the reason for the inversed contrast in Figure 4d relative to the TEM images of Figure 2. The length scale is unchanged in the two cases. Figure 4e shows a TEM image from sample's margin where the copper gyroid scaffold is very clear. Now, the TEM imaging was made several weeks after the electrodeposition experiment. The sample was kept in air in the mean time, in which case copper is expected to oxidize.[28] The crystalline patterns in the high-resolution TEM images of Figures S5 and S6 show periodicity of 2.54 ± 0.06 Å, consistent with the d_{111} crystal spacing observed in nanoparticles of cuprite, Cu_2O, from in-air-oxidized copper nanoparticles.[28]

In conclusion, we have presented a simple method for generating hydrophilic nanoporous materials of conserved nanostructure by photooxidation in air of hydrophobic nanoporous polymers. The vast knowledge on photooxidation of polymers accumulated in the field of polymer degradation is expected to play a constructive role within the method presented. The typical chemical groups responsible for the hydrophilicity are carboxyl and hydroxyl groups. Hydrophilic patterns of few micrometer length scale were easily produced. Conversely, it was argued that nanoporous polymers constitute unique model materials for the study of the general phenomenon of polymer photooxidation.

The overall method presented combines molecular self-organization as a bottom-up procedure for the production of nanoporous polymers with UV patterning as a top-down procedure for changing the chemical composition of the concentrated polymer−air interface. A number of added and structure-related physicochemical properties such as water self-confinement and flow, refractive index contrast, large surface area, accessible chemically reactive functional groups, and nanoporosity can be combined to generate a multitude of new application possibilities.

Acknowledgment. We thank Mogens H. Jakobsen and Gabriella Blagoi (DTU Nanotech) for permission to use their UV reactor, Jens W. Andreasen (Risø-DTU) for assistance with SAXS, Niels B. Larsen (DTU Nanotech) for providing the lithographic UV masks, and Kell Mortensen (KU-Life, University of Copenhagen) for useful discussions. We acknowledge the financial support from the Danish Research Agency for Technology and Production.

Supporting Information Available: Figures S1−S6. This material is available free of charge via the Internet at http://pubs.acs.org.

References and Notes

(1) Rabek, J. F. *Polymer Photodegradation*; Chapman & Hall: London, 1995; Chapters 1−3.
(2) Rabek, J. F. *Photodegradation of Polymers*; Springer: Berlin, 1996.
(3) Adam, C.; Lacoste, J.; Lemaire, J. *Polym. Degrad. Stab.* **1990**, *29*, 305.
(4) Piton, M.; Rivaton, A. *Polym. Degrad. Stab.* **1996**, *53*, 343.
(5) Lucki, J.; Ranby, B.; Rabek, J. F. *Eur. Polym. J.* **1979**, *15*, 1101.
(6) Vieth, W. R.; Howell, J. M.; Hsieh, J. H. *J. Membr. Sci.* **1976**, *1*, 177.
(7) Paul, D. R. *Phys. Chem. Chem. Phys.* **1979**, *83*, 294.
(8) Lee, J.-S.; Hirao, A.; Nakahama, S. *Macromolecules* **1988**, *21*, 274.
(9) Thurn-Albrecht, T.; Schotter, J.; Kastle, G. A.; Emley, N.; Shibauchi, T.; Krusin-Elbaum, L.; Guarini, K.; Black, C. T.; Tuominen, M. T.; Russell, T. P. *Science* **2000**, *290*, 2126.
(10) Yang, S. Y.; Ryu, I.; Kim, H. Y.; Kim, J. K.; Jang, S. K.; Russell, T. P. *Adv. Mater.* **2006**, *18*, 709.
(11) Urbas, A. M.; Maldovan, M.; DeRege, P.; Thomas, E. L. *Adv. Mater.* **2002**, *14*, 1850.
(12) Risk, W. P.; Kim, H. C.; Miller, R. D.; Temkin, H.; Gangopadhyay, S. *Opt. Express* **2004**, *12*, 6446.
(13) Hillmyer, M. A. *Adv. Polym. Sci.* **2005**, *190*, 137.
(14) Ndoni, S.; Vigild, M. E.; Berg, R. H. *J. Am. Chem. Soc.* **2003**, *125*, 13366.
(15) Bates, F. S.; Frederickson, G. H. *Annu. Rev. Phys. Chem.* **1990**, *41*, 525.

(16) We visually observe that 0.5 mm thick NP films of hexagonally packed cylindrical pores are opaque or translucent, despite structural length scales of ~20 nm. This might be due to birefringent light scattering from a multidomain material, with cylinder orientational domain size in the micrometer range. Shear aligned samples are more transparent.
(17) Guo, F.; Andreasen, J. W.; Vigild, M. E.; Ndoni, S. *Macromolecules* **2007**, *40*, 3669.
(18) Hajduk, D. A.; Harper, P. E.; Gruner, S. M.; Honeker, C. C.; Kim, G.; Thomas, E. L.; Fetters, L. J. *Macromolecules* **1994**, *27*, 4063.
(19) Kim, H.-C.; Kreller, C. R.; Tran, K. A.; Sisodiya, V.; Angelos, S.; Wallraff, G.; Swanson, S.; Miller, R. D. *Chem. Mater.* **2004**, *16*, 4267.
(20) Ndoni, S.; Papadakis, C. M.; Almdal, K.; Bates, F. S. *Rev. Sci. Instrum.* **1995**, *66*, 1090.
(21) Oxygen fixation on these highly cross-linked matrices should mainly happen at the interface; otherwise, a change in the length scale should be observed by SAXS. The free radicals formed in the process of photooxidation fix oxygen mostly at the air interface due to higher oxygen concentration in the pore volume than in the polymer bulk. At increasing irradiation times the oxidized layer expands into the matrix bulk.
(22) Ito, M.; Matsumoto, M.; Doi, M. *Fluid Phase Equilib.* **1998**, *144*, 395. A molecular dynamic simulation of O_2 permeation into a polyethylene film showing polymer−air interface enriched with O_2 and a sharp fall (within 1−2 nm) in O_2 concentration in the bulk; this can be relevant for the present situation.
(23) There are three relevant time scales in the process of NP photooxidation related to O_2 diffusion into the nanopores (τ_K), O_2 diffusion into the bulk polymer (τ_B), and O_2 consumption by photoreaction (τ_R). O_2 transport through the nanopores occurs by Knudsen diffusion. In the present case Knudsen diffusion coefficient is $\sim 10^6$ larger than bulk diffusion coefficient. For a given NP the mentioned characteristic times are sample thickness dependent, and they are expected to change in the course of photofixation due to material's chemical and optical property changes. In the present case the initial absorbance of UV is low so that photooxidation in the majority of the sample is expected initially to happen at conditions of quasi-equilibrium in oxygen concentration in the pores and in the bulk, $\tau_K \leq \tau_B \ll \tau_R$. The bulk concentration can be taken equal to O_2 solubility in the polymer matrix, which in the present case is expected to be 10−20 times lower than O_2 concentration in air.
(24) The possibility of a special role in oxygen photofixation of in situ generated photoinitiator (benzophenone, one of the scission products of dicumyl peroxide during the oxygen-free cross-linking reaction) was excluded by the observation that the sample series cross-linked by the aliphatic diamyl peroxide showed the same behaviour under UV treatment as the DCP series.
(25) Li, L. Surface Modification of Nanoporous 1,2-Polybutadiene Matrices by Near UV-Induced Photooxidation, M.Sc. Thesis, Technical University of Denmark, **2007**.
(26) Larsson, A.; Dérand, H. *J. Colloid Interface Sci.* **2002**, *246*, 214.
(27) The estimated refractive index at 633 nm is 1.30 for the dry NP and 1.43 for the water-filled NP. The edges of the hydrophilic pattern visibly scatter light due to roughness of length scale ~1−10 μm, conveyed from the "coarse" aluminum UV mask during the patterning process.
(28) Urban, J.; Sack-Kongehl, H.; Hweiss, K. *Z. Phys. D* **1995**, *36*, 73.